

SUPPLEMENTAL DATA**Experimental Procedures**

Construct Design—Plasmids pGEX-4T1-Ufd2, pGEX-4T1-Rad23, and pGEX-Dsk2 for the expression of N-terminally GST-tagged *Saccharomyces cerevisiae* Ufd2, Rad23, and Dsk2 were kindly provided by Stefan Jentsch. The UBL domains of Rad23 (aa 1-84) and Dsk2 (aa 1-79 and aa 1-84) were PCR amplified and inserted into the pET21b vector (Novagen, C-terminal His-tag, NdeI/BamHI). N-terminal His-tagged Rad23-UBL (aa 1-74) and Dsk2-UBL (aa 1-74) were cloned additionally from chromosomal DNA into the vector pETM11 (EMBL Heidelberg, NcoI/XhoI). C-terminal GST-tagged Ufd2 expression plasmid: The open reading frame (ORF) of Ufd2 was PCR amplified and inserted into the pET3a-GST plasmid (NdeI/ApaI). The pET3a-GST plasmid was generated by cloning the GST-encoding ORF of pGEX-4T1 (GE-Healthcare) into the pET3a vector (Novagen, ApaI/BamHI) (Sven Eiselein). C-terminally GST-tagged Ufd2 was used to compare and validate the optimal binding of N-terminally GST-tagged Ufd2 with the UBL domains in the SPR interaction studies. For cloning of the *Schizosaccharomyces pombe* homolog of Ufd2 and the UBL domains of SpRad23 (Rhp23) and SpDsk2 (Dph1), *S. pombe* cDNA was prepared by reverse transcription. The fragments encoding for UBLs as well as the ORF of Ufd2 were amplified and inserted into pET21b (Novagen, NdeI/BamHI) or pET3a-GST (NdeI/ApaI), respectively.

Protein Expression and Purification—All proteins were expressed in *E. coli* BL21(DE3) RIL cells (Novagen). GST-Ufd2 was expressed after heat shock at 42°C for 30 minutes and by induction at an OD₆₀₀ = 0.6 with 0.01 mM IPTG (isopropyl-β-thiogalactoside) at 16°C for 40 h. His₆ tagged Rad23-UBL and Dsk2-UBL proteins were expressed by induction at an OD₆₀₀ = 0.6 with 0.4 mM IPTG at 37°C for 4-5 h.

Untagged Ufd2 was purified in PBS buffer by affinity chromatography using immobilized glutathione (GST•Bind Resin, Novagen) followed by overnight on-column cleavage with

UBL-Binding Domain of Ufd2

thrombin at 16 °C and size-exclusion chromatography (HiLoad 26/60 Superdex 200 prep grade, GE Healthcare) or (High performance Superdex 200 10/300 GL) in 50 mM HEPES pH 7.4, 150 mM NaCl and 1 mM β-mercaptoethanol.

For GST pull-down and comparative SPR binding studies, GST-tagged Ufd2 was eluted from the GSH column with 20 mM reduced glutathione and desalted either by size-exclusion chromatography on Sephadex G-25 equilibrated with 50 mM HEPES pH 7.4, 150 mM NaCl and 1 mM β-mercaptoethanol or using U-tube concentrators (Novagen).

Rad23- and Dsk2-UBL domains were purified in sodium phosphate buffer by metal affinity chromatography (Ni-NTA, Invitrogen) followed by size-exclusion chromatography (HiLoad 26/60 Superdex 200 prep grade, GE Healthcare) in 50 mM HEPES pH 7.4, 150 mM NaCl and 1 mM β-mercaptoethanol. All proteins were concentrated to ~20 mg/ml by ultrafiltration (Vivaspin, Sartorius), shock frozen, and stored at -80 °C.

Site Directed Mutagenesis—For site directed mutagenesis the QuikChange® II Site-Directed Mutagenesis Kit from Stratagene was used. The following mutants were created: (a) pGEX-4T1-Ufd2: E26A, D40A, L44A, E49A, R92A, G96A, V100A, I104A, F107A, T48A, Y97A, L44A/F107A, E26A/E49A, R92A/G96A, and V100A/I104A (b) pET21b-Rad23-UBL (C-terminal His-tag): F9A, K10A, I45A, S47A, G48A, V50A, Q52A, Q67A, V69A, M71A, I45A/V69A, S47A/G48A, F9A/K10A, V50A/M71A, Q52A/Q67A, and S47A/V50A (c) pET21b-Dsk2-UBL (C-terminal His-tag): G10F/Q11K/S67Q/H69V/V71M, and G10F/Q11K/I50V/K52Q/S67Q/H69V/V71M.

UBL-Binding Domain of Ufd2

SUPPLEMENTAL TABLE 1

Data collection

	Ufd2:Rad23-UBL	Ufd2:Dsk2-UBL
Data Collection		
Resolution (Å)	45.5-2.4 (2.53-2.4)	73.5-2.4 (2.53-2.4)
Wavelength (Å)	0.9	0.976
Space group	<i>P</i> 2 ₁ 2 ₁ 2 ₁	<i>P</i> 2 ₁ 2 ₁ 2 ₁
Cell dimensions (Å)	<i>a</i> = 65.0, <i>b</i> = 126.6, <i>c</i> = 180.9	<i>a</i> = 65.1, <i>b</i> = 125.7, <i>c</i> = 181.2
Unique reflections	59,314	58,089
<i><I/σI></i>	15.6 (3.3)	12.9 (2.2)
Completeness (%)	100 (100)	98.6 (95.1)
Redundancy	5.1 (5.2)	3.8 (3.5)
<i>R</i> _{sym}	0.070 (0.492)	0.062 (0.509)

Numbers in parentheses refer to the respective highest resolution data shell in each data set. $R_{\text{sym}} = \frac{\sum_{\text{hkl}} \sum_i |I_i - \langle I \rangle|}{\sum_{\text{hkl}} \sum_i \langle I \rangle}$ where I_i is the i^{th} measurement and $\langle I \rangle$ is the weighted mean of all measurements of I . $\langle I/\sigma I \rangle$ indicates the average of the intensity divided by its average standard deviation.

SUPPLEMENTAL TABLE 2

ITC parameters of Ufd2, Rad23-UBL, Dsk2-UBL and variants

	K_d	Fold	N	ΔH (kcal/mol)	$-\Delta S$ (kcal/mol, T=298 K)	ΔG (kcal/mol)
decrease						
Ufd2-wt	wt-Rad23-UBL	70 nM	0.68	-17.3	7.4	-9.8
	wt-Dsk2-UBL	175 nM	0.80	-10.1	0.8	-9.3
Ufd2-E26A	wt-Rad23-UBL	284 nM	4	0.91	-8.1	-8.9
	wt-Dsk2-UBL	521 nM	3	0.75	-7.3	-8.6
Ufd2-D40A	wt-Rad23-UBL	7.9 μ M	110	0.55	-19.7	12.7
	wt-Dsk2-UBL	7.6 μ M	40	1 ^a	-7.6	0.6
Ufd2-L44A	wt-Rad23-UBL	8.3 μ M	120	0.22	-29.7	22.8
	wt-Dsk2-UBL	463 nM	3	0.78	-10.1	1.5
Ufd2-T48A	wt-Rad23-UBL	72 nM	=	0.76	-12.1	2.3
	wt-Dsk2-UBL	296 nM	2	0.75	-10.7	1.8
Ufd2-E49A	wt-Rad23-UBL	413 nM	6	0.81	-11.2	2.5
	wt-Dsk2-UBL	314 nM	2	0.80	-8.6	-0.2
Ufd2-R92A	wt-Rad23-UBL	265 nM	4	0.65	-3.4	-5.6
	wt-Dsk2-UBL	128 nM	=	0.73	-7.8	-1.6
Ufd2-G96A	wt-Rad23-UBL	592 nM	8	0.72	-7.0	-1.5
	wt-Dsk2-UBL	216 nM	=	0.72	-13.2	4.1
Ufd2-Y97A	wt-Rad23-UBL	134 μ M	1900	1 ^a	-21.4	16.1

UBL-Binding Domain of Ufd2

Ufd2-V100A	wt-Dsk2-UBL	83 μM	470	1 ^a	-2.5	19.9	-5.6	
	wt-Rad23-UBL	n.d.	>10000	n.d.	n.d.	n.d.	n.d.	
	wt-Dsk2-UBL	3.9 μM	20	0.61	-10.6	3.2	-7.4	
Ufd2-I1104A	wt-Rad23-UBL	1.6 μM	20	0.96	-12.6	4.7	-7.9	
	wt-Dsk2-UBL	1.1 μM	6	0.87	-18.3	10.2	-8.1	
Ufd2-F107A	wt-Rad23-UBL	n.d.	>10000	n.d.	n.d.	n.d.	n.d.	
	wt-Dsk2-UBL	3.6 μM	20	0.60	-8.3	0.9	-7.4	
wt-Ufd2	Rad23-UBL-F9A	376 nM	5	0.94	-8.7	0.0	-8.8	
wt-Ufd2	Rad23-UBL-K10A	162 nM	2	0.85	-9.4	-0.2	-9.6	
wt-Ufd2	Rad23-UBL-I45A	9.1 μM	130	0.37	-19.1	12.2	-6.9	
wt-Ufd2	Rad23-UBL-S47A	606 nM	9	0.76	-4.8	-3.7	-8.5	
wt-Ufd2	Rad23-UBL-V50A	441 nM	6	0.89	-12.6	3.9	-8.7	
wt-Ufd2	Rad23-UBL-Q52A	415 nM	6	0.74	-6.2	-2.5	-8.7	
wt-Ufd2	Rad23-UBL-Q67A	113 nM	2	0.78	-9.5	0.0	-9.5	
wt-Ufd2	Rad23-UBL-V69A	478 nM	7	0.89	-8.8	0.2	-8.6	
wt-Ufd2	Rad23-UBL-M71A	221 nM	3	0.85	-7.9	-1.2	-9.1	
wt-Ufd2	Dsk2-UBL-	240 nM	=	0.60	-2.5	-6.5	-9.0	
	G10F/Q11K/S67Q/							
	H69V/V71M							

^a N values were fixed to 1 before fitting the data to allow accurate determination of the other parameters. n.d. not detected. = indicates no change

SUPPLEMENTAL FIGURE LEGENDS

SUPPLEMENTAL FIGURE S1. Comparative SPR analysis for binding of Ufd2 to wild type Rad23-UBL and its variants.

His₆-tagged wt Rad23-UBL, its single (*A*, *B*) or double mutants (*C*) were captured on a Ni-NTA sensor chip to an equal response unit (100 RU) in each cycle and GST-Ufd2 was applied in the mobile phase. *D*, The relative binding responses of UBL-variants at the end of two-minute injections of GST-Ufd2 are measured and percent wt responses are presented (Table 2).

SUPPLEMENTAL FIGURE S2. Comparative SPR analysis for binding of Ufd2 variants to Rad23- and Dsk2-UBL.

His₆-tagged Rad23-UBL (*A*) or Dsk2-UBL (*B*) are captured on a Ni-NTA sensor chip and variants of GST-Ufd2 were applied in the mobile phase as indicated. Percent wt responses are shown in a bar graph in supplemental Fig. S4B and Table 2.

SUPPLEMENTAL FIGURE S3. ITC experiments with Ufd2, Rad23-UBL, Dsk2-UBL, and their variants. *A*, Wt-Ufd2 titrated with Rad23-UBL variants. *B*, Ufd2 variants titrated with wt-Rad23-UBL. *C*, Ufd2 variants titrated with wt-Dsk2-UBL. All experiments were performed under the same conditions and the measured binding enthalpies are plotted as a function of the molar ratio of Rad23-UBL/Dsk2-UBL to Ufd2. The resulting binding parameters are summarized in supplemental Table S2.

SUPPLEMENTAL FIGURE S4. Comparison of the Ufd2:Rad23-UBL and Ufd2:Dsk2-UBL interface regions. *A*, Superposition of the Ufd2:Rad23-UBL and Ufd2:Dsk2-UBL interface region with residues involved in interaction shown as sticks. The N-terminal binding domain of Ufd2 is colored in orange (Rad23 complex) and gray (Dsk2 complex), Rad23-UBL in green and Dsk2-UBL in yellow. *B*, Relative binding responses of Ufd2 variants to the Rad23- and Dsk2-UBL are shown in bar graphs.

UBL-Binding Domain of Ufd2

SUPPLEMENTAL FIGURE S5. Sequence alignment of *S. cerevisiae* Ufd2 and human Ufd2s

E4A and E4B. The secondary structure elements of *S. cerevisiae* Ufd2 assigned using DSSP (1) are labeled above the sequences. The alignment was performed using DaliLite (2) and the figure was prepared with ESPript (3). Strictly conserved amino acids are highlighted with white letters in red and similar amino acids are in red letters. Residues colored in red represent the core region of the Ufd2:Rad23-UBL binding domain, which is essential for UBL interaction, while yellow shaded residues contribute moderately to the interaction.

References

1. Kabsch, W., and Sander, C. (1983) *Biopolymers* **22**, 2577-2637
2. Holm, L., Kaariainen, S., Rosenstrom, P., and Schenkel, A. (2008) *Bioinformatics* **24**, 2780-2781
3. Gouet, P., Courcelle, E., Stuart, D. I., and Metoz, F. (1999) *Bioinformatics* **15**, 305-308

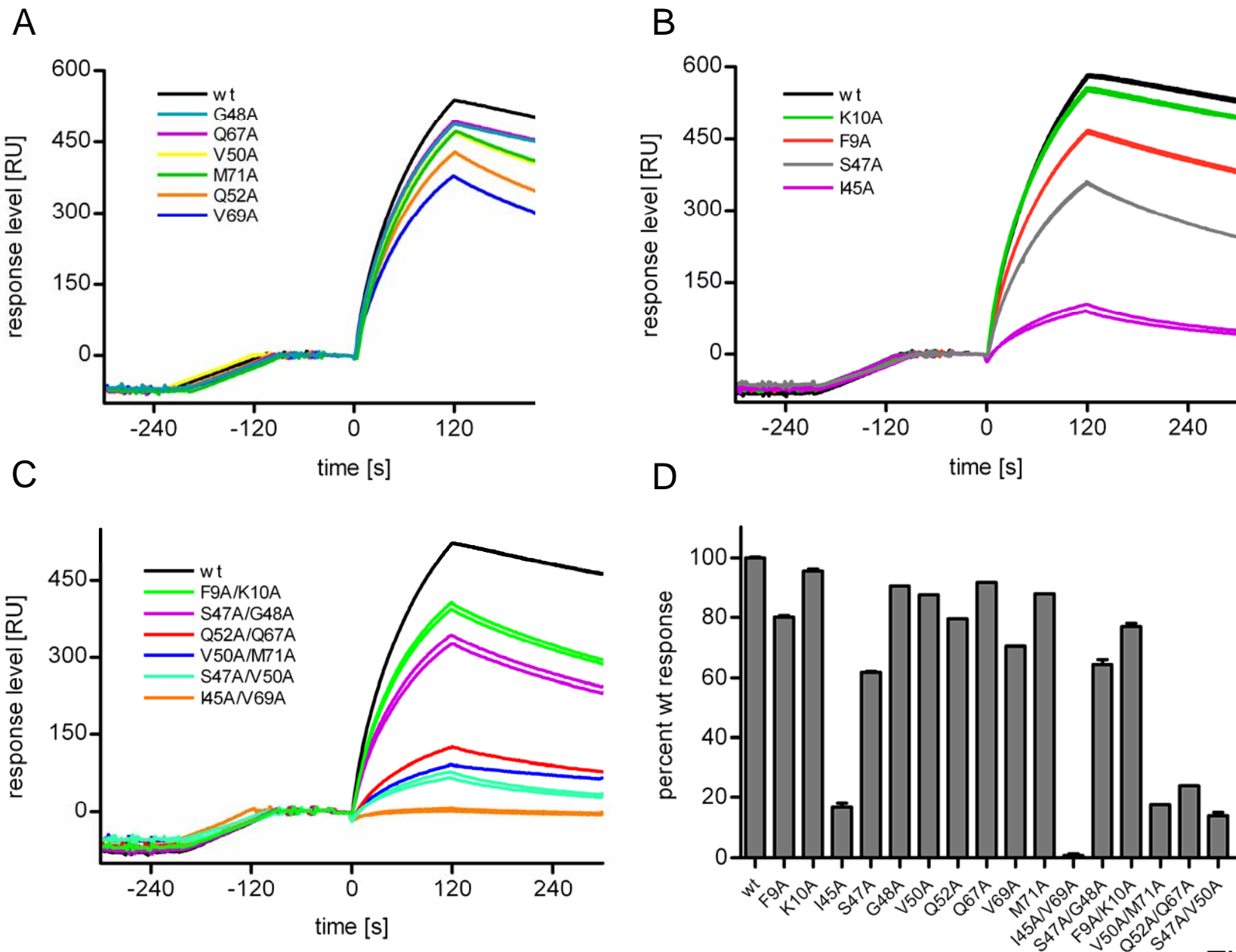
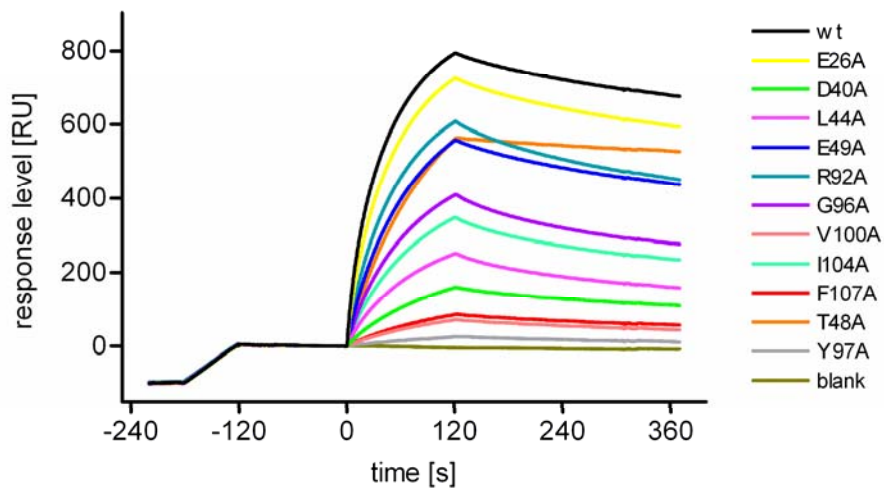


Figure S1

A



B

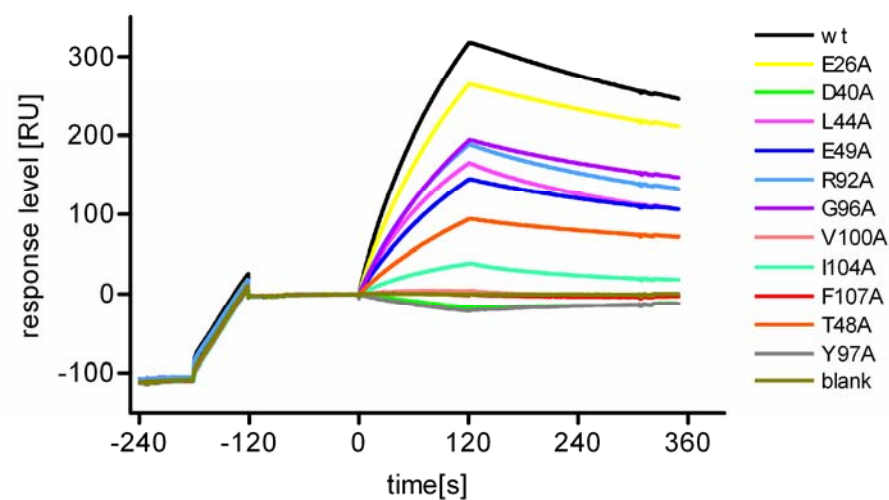


Figure S2

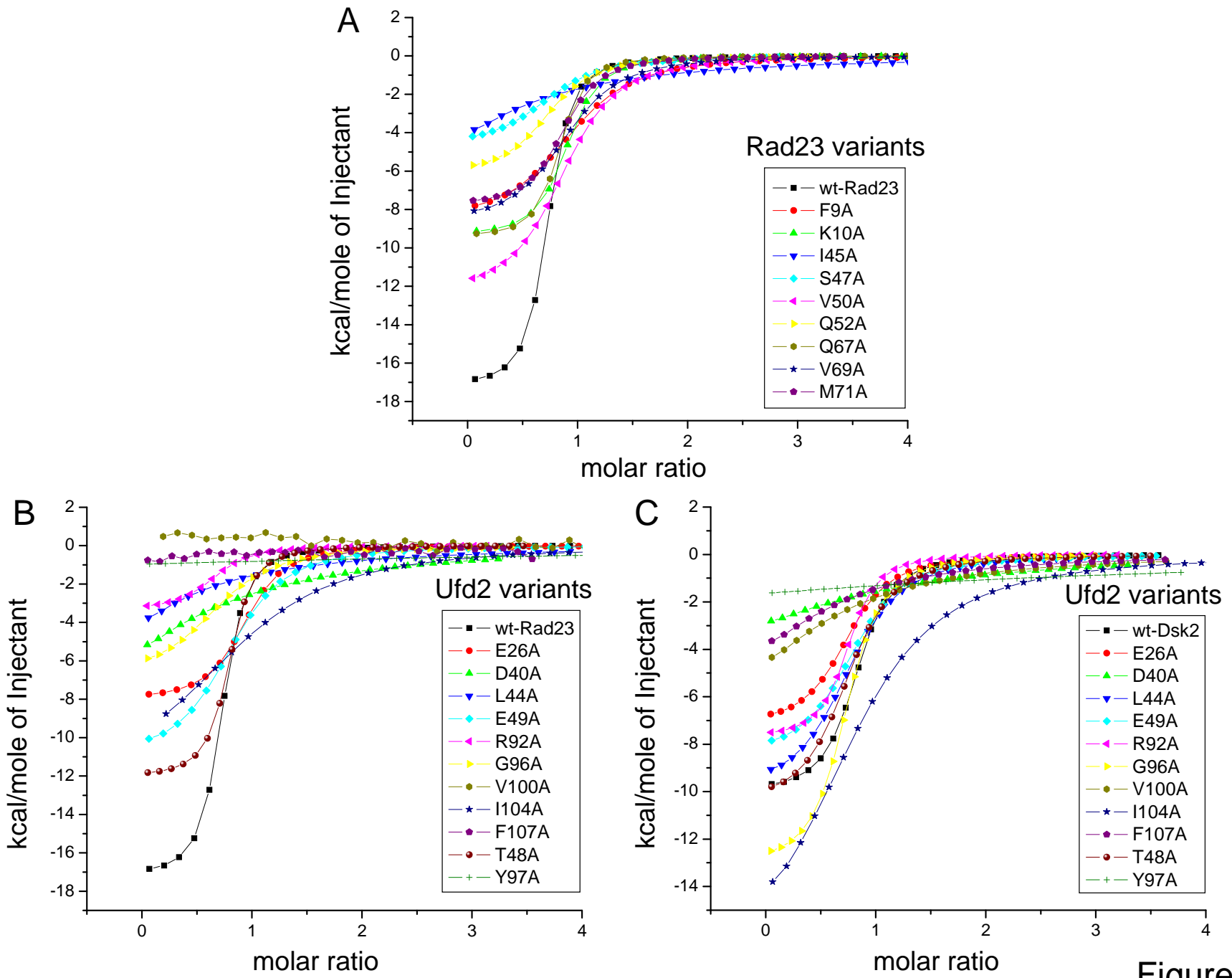
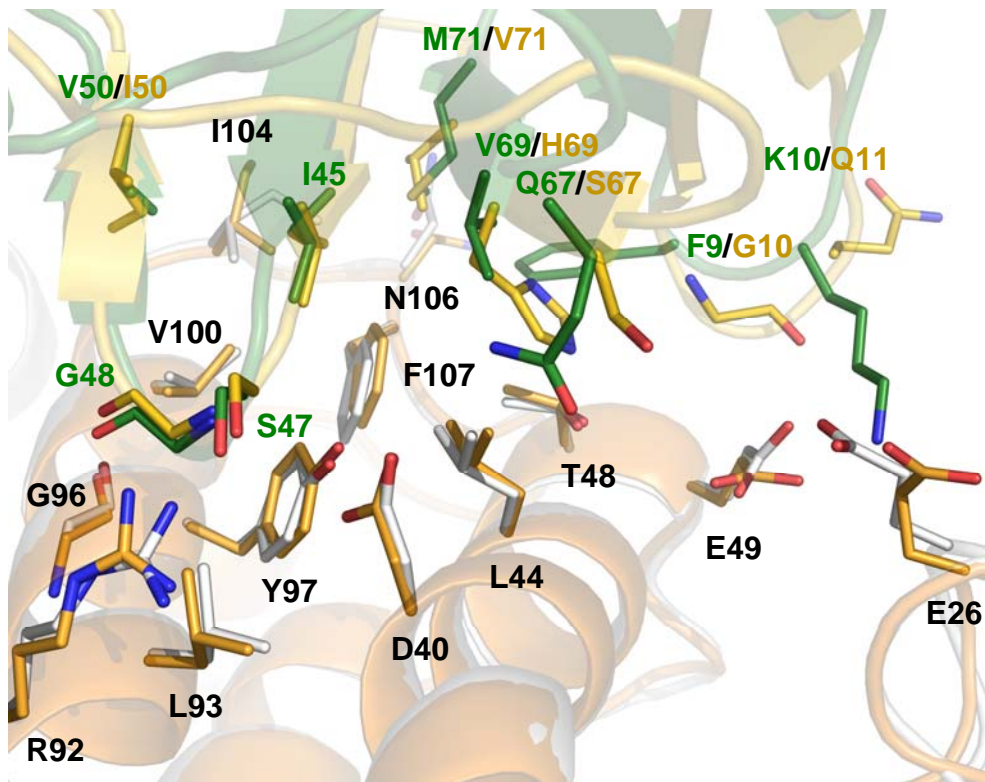


Figure S3

A



B

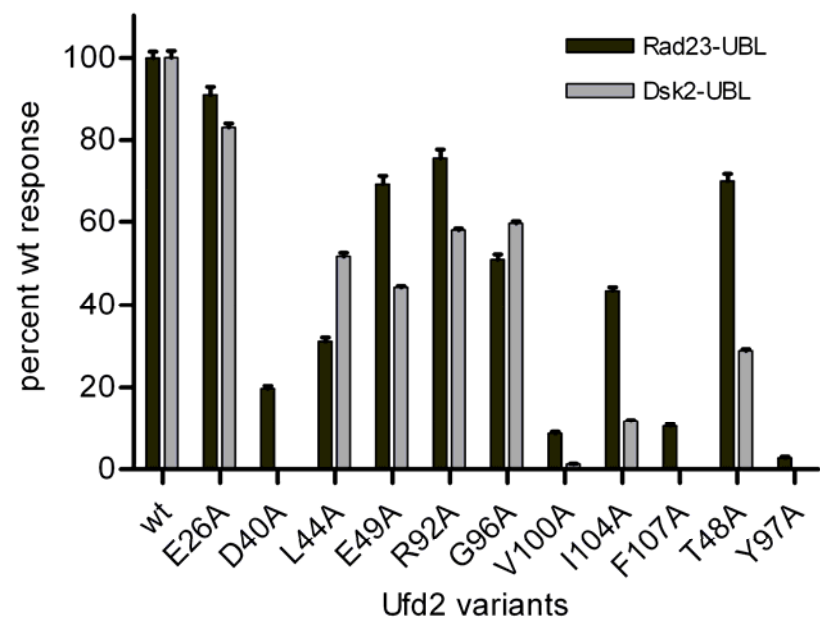


Figure S4

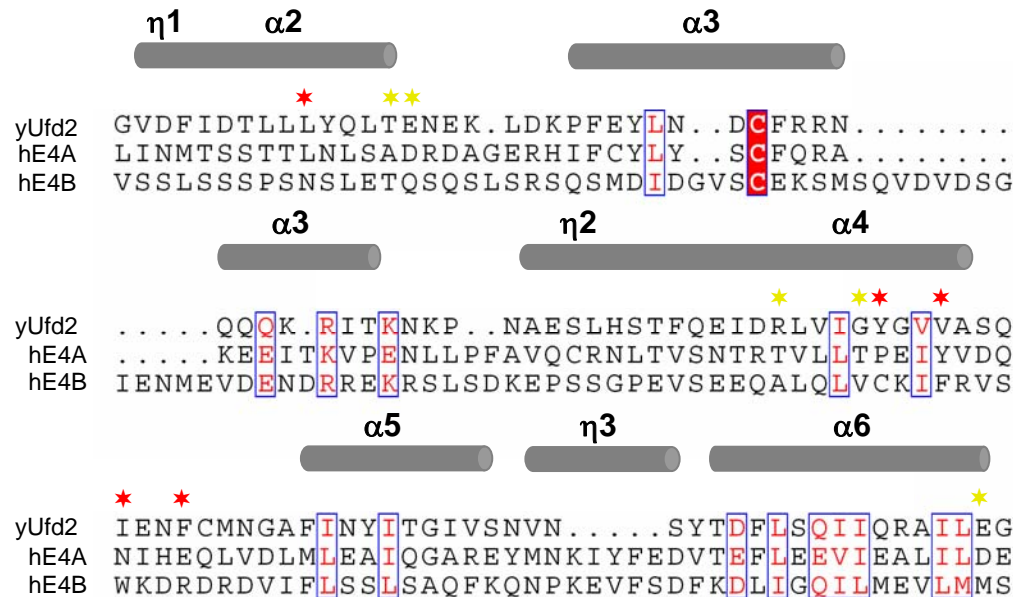


Figure S5